Analyzing powers for $^1\vec{\mathrm{H}}(\pi^+,\pi^+p)$ at $T_\pi=165$ and 240 MeV

B. A. Raue,[1] T. A. Greco,[1] M. G. Khayat,[2,*] F. Adimi,[2,†] B. van den Brandt,[7] H. Breuer,[2] T. Chang,[4] N. S. Chant,[2] H. Chen,[5] T. A. Dooling,[1] A. P. Dvoredsky,[2,‡] B. S. Flanders[6], T. Gu[2], J. P. Haas,[4] P. Hautle,[7] J. Huffman,[2] J. J. Kelly,[2] A. Klein,[1] K. Koch,[7,§] J. A. Konter,[7] A. I. Kovalev,[7,‖] G. S. Kyle,[4] J. J. Lawrie,[8] Z. Lin,[4] S. Mango,[7] P. Markowitz,[2,¶] R. Meier,[3,**] T. Payerle,[2] S. Ritt,[3,††] P. G. Roos,[2] and M. Wang[4,‡‡]

[1]*Old Dominion University, Norfolk, Virginia 23529*

[2]*University of Maryland, College Park, Maryland 20742*

[3]*University of Karlsruhe, Karlsruhe, Germany*

[4]*New Mexico State University, Las Cruces, New Mexico 88003*

[5]*Towson State University, Towson, Maryland 21204*

[6]*American University, Washington, D.C. 20016*

[7]*Paul Scherrer Institute, CH-4232 Villigen PSI, Switzerland*

[8]*National Accelerator Centre, Faure, South Africa*

(Received 19 October 1995)

We have measured the analyzing power for elastic scattering of π^+ from a target of polarized ^{1}H. Data were taken for incident pion beam energies of 165 and 240 MeV at several pion scattering angles. The current data generally agree with previously existing measurements of A_y for this reaction and also with results of the SAID phase-shift analysis program. In most cases the new data are of higher precision than previously existing data.

PACS number(s): 13.75.Gx, 24.70.+s, 25.80Dj

We have measured the analyzing powers for elastic scattering of π^+ from polarized ^{1}H for pion beam energies of $T_\pi=165$ and 240 MeV at several scattering angles. Previously reported results for beam energies near 165 MeV [1–3] do not extend to the small angles accessible to this experiment while previous results near 240 MeV [4,5] have relatively large uncertainties. The data presented here were acquired during two separate running periods at the Paul Scherrer Institute (PSI) in Villigen, Switzerland with very similar experimental setups. The main thrust of the first running period was to measure the analyzing power for the $^7\vec{\mathrm{Li}}(\pi^+,\pi^+p)$ reaction at $T_\pi=240$ MeV [6] while the second running period focused on measuring the $^7\vec{\mathrm{Li}}(\pi^+,pp)$ analyzing power at $T_\pi=165$ MeV [7]. Both experiments utilized a polarized ^{7}LiH target. The presence of polarized hydrogen in this target allowed us to gather $^1\vec{\mathrm{H}}(\pi^+,\pi^+p)$ analyzing power data along with the primary $^7\mathrm{Li}+\pi^+$ data. Initially, the $^1\vec{\mathrm{H}}(\pi^+,\pi^+p)$ data were analyzed to monitor stability of the target polarization. The high quality and internal consistency of these data prompted the writing of this Brief Report.

Central to the success of the ^{7}Li experiments was the development of the PSI polarized ^{7}LiH target [8]. The target consisted of chips of irradiated ^{7}LiH contained in an 18 mm wide by 18 mm high by 5 mm thick brass cavity. NMR coils were located in the median plane of the cavity to provide periodic monitoring of the target polarization. The cavity is held in the mixing chamber of a dilution refrigerator at the center of a 2.5 T magnetic field. The target was dynamically polarized yielding a positive polarization (normal to the scattering plane in the direction of the magnetic field) of hydrogen nuclei between 45 and 60 % and negative polarization between 40 and 50 %. The target polarization was determined to within an accuracy of $\pm4\%$ of the measured polarization value using the PSI NMR system [9]. During the 240 MeV running period, a single NMR coil measured the polarization of the ^{7}Li and the ^{1}H polarization was deduced using the equal spin temperature theory. For the 165 MeV running period, a second NMR coil provided a direct measurement of the ^{1}H polarization in addition to the direct measurement of the ^{7}Li polarization. The measured ^{1}H polarization and that deduced from the equal spin temperature theory, using the measured ^{7}Li polarization, are consistent within the uncertainties [7]. In addition to ^{7}Li and ^{1}H, the target also contained liquid ^{4}He and a small amount of ^{3}He (approximately 6%), necessary for the operation of the dilution refrigerator. During the 165 MeV running period, a thin CD_2 foil was located in front of the target cavity to provide calibration data.

---

*Present address: Kent State University, Kent, OH 44242.

†Present address: Saskatchewan Accelerator Laboratory, Saskatoon, Canada, SK S7N 5C6.

‡Present address: California Institute of Technology, Pasadena, CA 91125.

§Present address: Carinthian Institute of Technology, A-9800 Spittal/Drau, Austria.

‖Present address: St. Petersburg Nuclear Physics Institute, 188350 Gatchina, Russian Federation.

¶Present address: Florida International University, Miami, FL 33199.

**Present address: TRIUMF, Vancouver British Columbia, Canada V6T 2A3.

††Present address: University of Virginia, Charolettesville, VA 22901.

‡‡Present address: Applied Komatsu Technology America, Santa Clara, CA 95052.

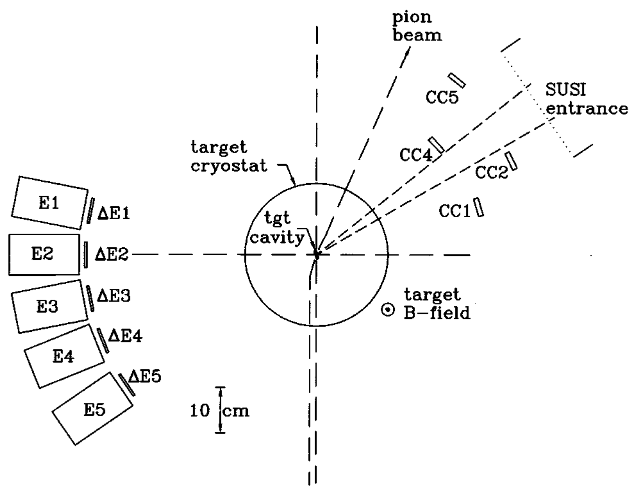

FIG. 1. Experimental apparatus setup in the PSI $\pi M1$ beamline. The pion beam is incident on a polarized ^{7}LiH target and bent by the target's magnetic field. The detectors include the SUSI spectrometer, four plastic-scintillator "complementary counters" (CC1-5), and five plastic-scintillator ΔE-E counters ($\Delta E1-5$ and $E1-5$), or "E blocks." The configuration shown is for the 165 MeV running period.

The experimental apparatus was based around the SUSI pion spectrometer in the PSI $\pi M1$ beamline [10] and is shown schematically in Fig. 1. In addition to the SUSI spectrometer, which was positioned at several different angles on the right side of the beam, we also viewed the target with five stacks of "E blocks" to the left of the beam and four "complementary counters" to the right of the beam. The E blocks each consisted of a 5.6-cm-wide by 12.7-cm-high by 0.5-cm-thick ΔE plastic scintillator followed by a 8.9 cm wide by 17.8 cm high by 15.2 cm thick plastic scintillator. The E blocks were mounted with the front face of the ΔE detector 50 cm from the target center. The complementary counters, CCs, were 4-cm-wide by 8.5-cm-high by 1-cm-thick plastic scintillators and were positioned between 35 and 45 cm from the target center. Both the E blocks and the CCs were on movable platforms that allowed for variation of the angles. The detector orientation shown in Fig. 1 is for the 165 MeV running period. During the 240 MeV running period, the E blocks were at more forward angles while the CCs and SUSI were at larger angles.

Nearly all of the data presented here are from coincident detection of pions and protons. Three combinations of detector coincidences were used; pions in SUSI coincident with protons in the E blocks, pions in the CCs with protons in the E blocks, and pions in E blocks with protons in the CCs. In the first case, scattered pions were identified in SUSI through momentum and time-of-flight cuts while standard ΔE-E techniques provided unambiguous identification of protons in the E blocks. In the second case, likely pion candidates were identified in the CCs through time-of-flight versus energy separation with protons again identified in the E blocks. In the last case, pions were identified in the E blocks through ΔE-E techniques with the likely proton candidates identified in the CCs through time-of-flight versus energy-loss separation. In all cases, the coincidence requirements placed stringent kinematical constraints on the collected data which assured clean identification of $\pi+p$ elastic scattering. Table I shows a breakdown of the energies, angles, and detector combinations used to collect the data.

TABLE I. Analyzing power at the different beam energies and scattering angles. The detector combinations are shown with the pion detector listed first followed by the proton detector. Analyzing power entries are followed by statistical and systematic errors respectively.

T_π (MeV)	$\Theta_{\text{c.m.}}$	A_y	Detector(s)
165	39.5	$0.182 \pm 0.019 \pm 0.008$	SUSI singles
	123.5	$0.107 \pm 0.072 \pm 0.007$	E block·CC
	142.8	$-0.06 \pm 0.11 \pm 0.003$	E block·CC
240	76.3	$0.391 \pm 0.008 \pm 0.016$	SUSI·E block
	99.3	$0.336 \pm 0.012 \pm 0.015$	CC·E block
	105.7	$0.318 \pm 0.020 \pm 0.015$	SUSI·E block
	106.1	$0.274 \pm 0.004 \pm 0.020$	CC·E block
	109.0	$0.212 \pm 0.010 \pm 0.019$	CC·E block
	123.5	$0.082 \pm 0.004 \pm 0.009$	CC·E block
	127.1	$0.047 \pm 0.012 \pm 0.004$	SUSI·E block
	134.5	$-0.011 \pm 0.009 \pm 0.001$	CC·E block

The power of the coincidence technique to cleanly identify $\pi+p$ elastic scattering is illustrated by the SUSI·E-block missing-energy spectrum shown in Fig. 2(a). In addition to the $\pi+p$ elastic scattering peak, the spectrum also has contributions arising from inelastic scattering from ^{7}Li and ^{4}He. These include peaks due to quasielastic proton knockout from ^{7}Li leading to the (unresolved) ground and first excited states of ^{6}He, quasielastic proton knockout from ^{4}He, and knockout of s-shell protons from ^{7}Li. The yield for each of these contributions was determined by fitting the missing-energy spectrum with appropriate line shapes utilizing the ALLFIT routine [11]. A small background function, which was determined by empty target runs, was included in the fit.

A single data point was taken (at $\theta_{\text{c.m.}}=39.5°$ and $T_\pi=165$ MeV) using SUSI in singles mode to detect the elastically scattered pions. As before, pions were identified through momentum and time-of-flight cuts. However, the identification of $\pi+p$ elastic scattering events was not as clean in this case due to the lack of coincidence information and to energy/momentum resolution insufficient to separate $\pi+p$ elastic data from pion scattering off other target materials. This includes contributions from pion elastic scattering off ^{2}H, ^{4}He, and ^{7}Li, and inelastic scattering from ^{7}Li to the ^{7}Li 4.6 MeV excited state as well as ^{7}Li breakup. The yield for each pion scattering reaction was determined by fitting the SUSI pion-energy spectra using the ALLFIT routine. A typical SUSI energy spectrum is shown in Fig. 2(b) along with the result of the lineshape fit. Yields from $\pi+{}^2$H elastic scattering and scattering to the 4.6 MeV excited state of ^{7}Li are small relative to the other reactions due to a low relative abundance of deuterium and a small relative cross section for the 4.6 MeV state [12]. Furthermore, these two peaks should appear in our spectrum at approximately the same energy, about 159 MeV. Therefore, no attempt was made to separate these contributions in the fit and thus appear as a single broad peak in the fitted SUSI energy spec-

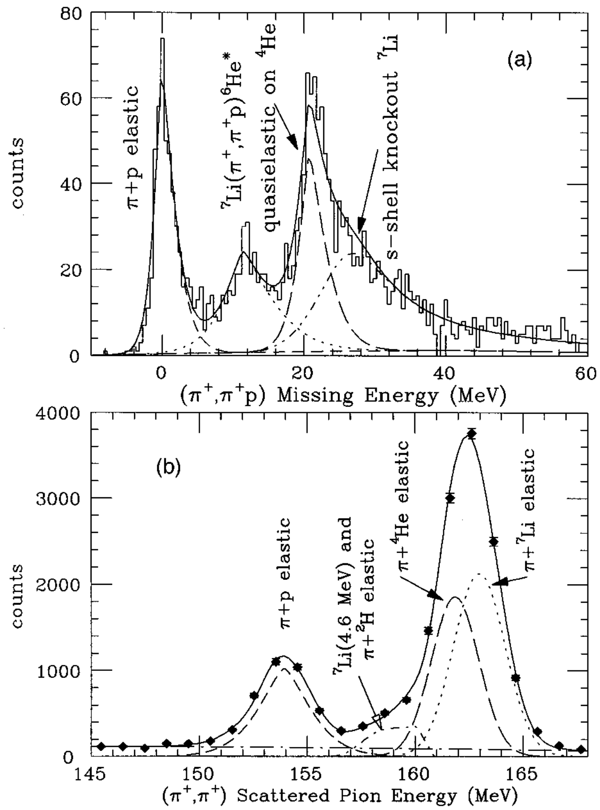

FIG. 2. (a) Typical missing-energy spectrum for pions detected in SUSI at $\theta_{\text{c.m.}}=76.3°$ in coincidence with protons in an E block for $T_\pi=240$ MeV. The curves represent the fitted yields for elastic pion scattering from ^{1}H (short dashes), quasielastic proton knockout from ^{7}Li to the ground and first excited states of ^{6}He (dots), quasielastic proton knockout from ^{4}He (long dashes), knockout of s-shell protons from ^{7}Li (dot-dot-dash), and the sum of the yields (solid). (b) Typical SUSI energy spectrum (data points) for $\theta_{\text{c.m.}}=39.5°$ and $T_\pi=165$ MeV. The lines represent the fitted yields for elastic pion scattering from ^{1}H (short dashes), ^{4}He (long dashes), and ^{7}Li (dots), a combination of inelastic scattering to the 4.6 MeV excited state of ^{7}Li and elastic scattering from ^{2}H (dot-dot-dash), quasielastic $\pi+p$ from ^{7}Li (dot-dash), and the sum of the yields (solid).

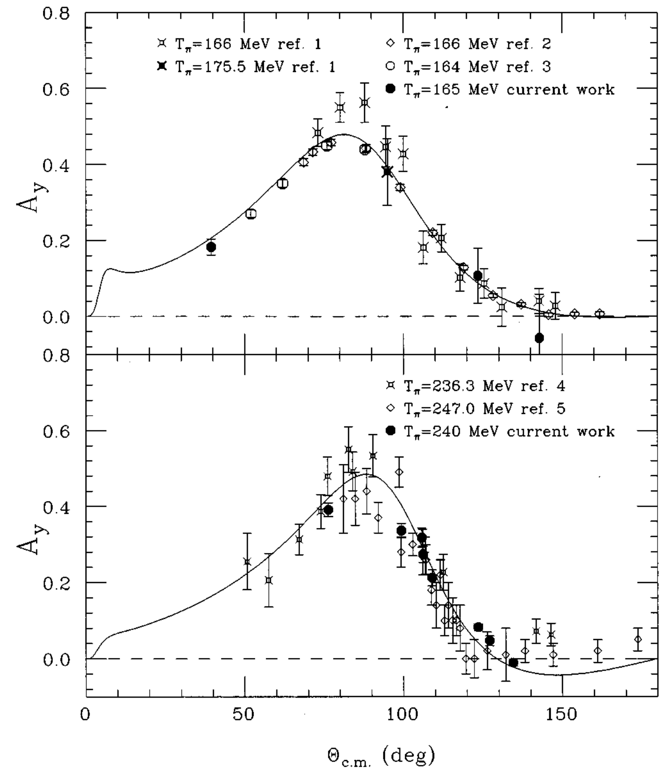

FIG. 3. Analyzing power versus center-of-mass scattering angle of the pion for $^1\vec{\text{H}}(\pi^+,\pi^+p)$ at $T_\pi=165$ (top) and 240 MeV (bottom) along with previously existing data and results from SAID [13]. Error bars on the current data are the quadrature sum of statistical and systematic uncertainties.

trum. The energy separations of all fitted peaks agree well with what is expected from kinematics, though there is a slight (0.5 MeV) overall shift to smaller energies due to an energy calibration offset. What appears to be a uniform background in the energy spectrum has a peak centroid and width consistent, within our energy acceptance and resolution, with quasielastic $^7\text{Li}(\pi^+,\pi^+p)$ smeared by Fermi motion.

The analyzing power data is shown in Table I and plotted in Fig. 3 along with the previously existing data and the results from the phase-shift analysis program SAID [13]. The error bars shown in the plot of the current data are the statistical and systematic uncertainties added in quadrature. The systematic uncertainties are the quadrature sum of contributions from uncertainties in the target polarization, detector angles, beam position, and beam energy. The statistical uncertainty for the point at $\theta_{\text{c.m.}}=39.5°$ and $T_\pi=165$ MeV takes into account the fitting errors of the SUSI pion-energy spectrum.

Most of the data presented here have significantly smaller uncertainties than previously reported results at similar beam energies [1–5] or provide data at previously unmeasured angles. At $T_\pi=165$ MeV, the data points at 123.5° and 142.8° have relatively large uncertainties but do confirm the existing data base. They also enhance confidence in the validity of our experimental technique. The point at 39.5° stands out in that it is the smallest angle datum at present, and nicely confirms the trend of the data of Ref. [3]. The data at $T_\pi=240$ MeV have uncertainties which are a factor of 3 to 4 smaller than previous data at similar energies. Within the uncertainties, the new data agree well with the previous measurements and are in good agreement with the predictions generated by SAID. These new data should provide improvement to the precision of the existing $\pi+p$ scattering data base.

We would like to thank G. Durand for kindly providing the chips of ^{7}LiH which were irradiated at Saclay.

[1] C. Amsler, L. Dubal, G. H. Eaton, R. Frosch, S. Mango, F. Požar, and U. Rohrer, Lett. Nuovo Cimento **15**, 209 (1976).

[2] M. E. Sevior *et al.*, Phys. Rev. C **40**, 2780 (1989).

[3] R. Meier *et al.*, Phys. Rev. C **42**, 2222 (1990).

[4] C. Amsler, F. Rudolf, P. Weymuth, L. Dubal, G. H. Eaton, R. Frosch, S. Mango, and F. Požar, Phys. Lett. **57B**, 289 (1975).

[5] W. Gorn, C. C. Morehouse, T. Powell, P. R. Robrish, S. Rock, S. Shannon, H. M. Steiner, and H. Weisberg, Bull. Am. Phys. Soc. **12**, 469 (1967).

[6] M. G. Khayat, Ph.D. thesis, University of Maryland, 1995; M. G. Khayat *et al.*, Bull. Am. Phys. Soc. **39**, 1391 (1994).

[7] T. A. Greco, Ph.D. thesis, Old Dominion University, 1995; T. Greco *et al.*, Bull. Am. Phys. Soc. **39**, 1391 (1994).

[8] B. van den Brandt, J. A. Konter, A. I. Kovalev, S. Mango, and M. Wessler, in *Proceedings of the 10th International Symposium on High Energy Physics, Frontiers of High Energy Spin Physics*, Nagoya, Japan, 1992, edited by T. Hasegaw, N. Horikawa, A. Masaike, and S. Sawada (Universal Academy, Tokyo, Japan, 1993), p. 369; B. van den Brandt, J. A. Konter, A. I. Kovalev, S. Mango, and M. Wessler, Paul Scherrer Institut Nuclear and Particle Physics Newsletter, Annex I Annual Report, 1992, p. 19.

[9] M. Wessler, J. Böhler, B. van den Brandt, J. A. Konter, and S. Mango, in *High Energy Spin Physics, Volume 2: Workshops, Proceedings of the IX International Symposium*, 6th Workshop on Polarized Solid Targets, Bonn, Germany 1990, edited by W. Meyer, E. Steffens, and W. Thiel (Springer-Verlag, Berlin, 1991) p. 277.

[10] R. Balsiger *et al.*, Nucl. Instrum. Methods **157**, 247 (1978); Swiss Institute for Nuclear Research User's Handbook, 1981, p. 64.

[11] J. J. Kelly, computer program ALLFIT (unpublished).

[12] R. Meier *et al.*, Phys. Rev. C **49**, 320 (1994).

[13] R. A. Arndt and L. O. Roper, SAID Phase Shift Analysis Program, results from Oct. 17, 1995.